Journal of Fluids and Structures (2000) **14,** 669–690
doi:10.1006/jfls.2000.0288 available online at http://www.idealibrary.com on IDEAL®

VIBRATIONS OF CIRCULAR CYLINDRICAL SHELLS WITH NONUNIFORM CONSTRAINTS, ELASTIC BED AND ADDED MASS; PART I: EMPTY AND FLUID-FILLED SHELLS

M. Amabili and R. Garziera

Dipartimento di Ingegneria Industriale, Università di Parma, Parco Area delle Scienze 181/A Parma, I - 43100 Italy

(Received 21 May 1999, and in final form 26 October 2000)

Circular cylindrical shells with nonuniform edge constraints (with zero radial and circumferential displacement) are investigated, including riveted shells. The linear modes of simply supported shells vibrating *in vacuo* are used as admissible functions, and the solution is obtained with the artificial spring method. The Flügge theory of shells is used and in-plane inertia is retained. Any shell constraint other than simple supports can be studied with the proposed method. Complicating effects due to the contained inviscid fluid, elastic bed of partial axial and angular dimensions, intermediate constraints and added mass are considered. The convergence of the method is numerically investigated and the effect of the number of rivets (clamped arcs) on shell modes is studied.

1. INTRODUCTION

The application of the Rayleigh–Ritz method to structures with rigid boundaries by treating such problems as limiting cases of free boundary problems, for which the admissible functions can be simpler, has largely extended the power of the method. This technique introduces artificial translational and rotational springs at the boundaries; the stiffness of these springs can be assumed sufficiently high to simulate rigid constraints with the required accuracy. Recent applications of this technique to shells were made, e.g. by Yuan & Dickinson (1994), Cheng and Nicolas (1992), Cheng (1994) and Amabili *et al.* (1998).

The Rayleigh–Ritz method estimates natural frequencies as an upper-bound value as a consequence of the discretization of the system. When artificial springs are used, the structure studied is a little more flexible than the original one, and natural frequencies can be underestimated. However, Ilanko and Dickinson (1999) have shown that if a negative stiffness is used for the artificial springs, natural frequencies are overestimated. Therefore, computing natural frequencies for both positive and negative stiffnesses, gives a measure of the accuracy reached, excluding the truncation effect due to discretization.

Amabili and Garziera (1999) proposed to use in the Rayleigh–Ritz method a simple and systematic choice of admissible functions which are the eigenfunctions of the closest, simple problem extracted from the one considered. In particular, the problem extracted must be "less constrained" than the original one; what is meant by less constrained is a problem where some constraints or other complications (e.g. added masses) are eliminated. The rigid constraints eliminated are replaced by elastic ones. The convergence of the method has been analytically investigated.

0889–9746/00/070669 + 22 $35.00/0

The present study is the application of the systematic choice of admissible functions in the Rayleigh–Ritz method developed by Amabili & Garziera (1999) to a quite complex problem in which a circular cylindrical shell presents nonuniform edge constraints (with zero radial and circumferential displacement). The possibility of having discontinuous constraints as for riveted shells is also studied. The linear modes of simply supported shells vibrating *in vacuo* are used as admissible functions; this case will be considered as the simple problem extracted from the one under study. Therefore, any shell constraint other than simple supports can be studied with the proposed method. Moreover, the following complicating effects are considered: a contained inviscid fluid, elastic bed of partial longitudinal and angular dimension, intermediate constraints and added mass. Part II of the present study will investigate vibrations of shells coupled to flowing fluid. The present study is related to that of Amabili *et al.* (1997), where circular plates with nonuniform constraints have been studied by using the same method. In particular, the Flügge theory of shells is used and in-plane inertia is retained. Each complicating effect adds an additional matrix to the original eigenvalue problem; this additional matrix can be built separately, without complicating the solution of the whole problem. The number of degrees of freedom, i.e. the dimension of the eigenvalue problem, is largely reduced with respect to other numerical approaches, like the finite element method.

Many interesting studies are available for circular cylindrical shells with uniform edge constraints. A very well-known study is Forsberg's (1964) that investigated the influence of uniform boundary conditions on natural frequencies. Additional works up to the 1960s are reviewed in Leissa's (1973) book. Recently, Loveday & Rogers (1998) studied free vibrations of elastically supported circular cylindrical shells by using the Flügge theory of shells. They investigated the effect on natural frequencies of translational and rotational springs with uniform stiffness around each shell edge.

Non-uniform boundary conditions have been studied for circular plates, e.g. by Amabili *et al.* (1997), Leissa *et al.* (1979); analogous study for circular shells is less extensive. Nonlinear vibrations of laminated circular cylindrical shells with nonuniform rotational edge constraints have been studied by Fu and Chia (1993). They analysed a shell with nonuniform boundary conditions with a discontinuous variation, i.e. built-in on an arc and simply supported on the following arc. No constraint on the axial displacement was imposed. The solution was obtained by using a double Fourier series expansion, but few terms were retained due to the complexity of the nonlinear shell theory used.

Circular shells partially loaded by a distributed mass and resting on an elastic bed have been studied by Amabili and Dalpiaz (1997). Both the mass load and the elastic bed were assumed to be applied on limited arcs and with arbitrary distributions in the circumferential direction, while they were considered to be uniformly distributed in the axial direction on the entire shell length.

The effect of lumped masses on the free vibrations of empty and fluid-filled shells has been studied theoretically, by using the receptance method, and experimentally by Amabili (1996); the effect of a single lumped mass on a cylindrical panel has been studied by Soedel (1993) using the receptance method.

Internal uniform constraints have been studied in several papers. For example, Païdoussis and Lakis (1972) studied vibrations of circular cylindrical shells with several axially equispaced constraints. However, nonuniform internal line and surface constraints are more complex and can be studied by using the present method.

2. SHELL WITH NONUNIFORM CONSTRAINTS

A cylindrical coordinate system $(O; x, r, \theta)$ is introduced, with the origin O at the centre of the shell edge. The circular cylindrical shell has radius R, length L and uniform thickness h,

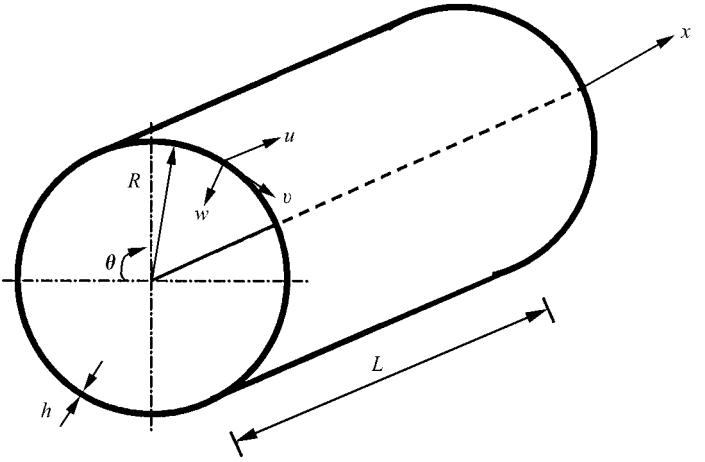

Figure 1. Schematic of the shell, coordinate system and shell displacements.

and the displacement of a point on the mean surface in the axial, angular and radial directions is indicated by u, v and w, respectively (see Figure 1). The mode shapes of the shell are expanded by using a base involving all the linear modes of the simply supported shell vibrating *in vacuo*; this case will be considered as the simple problem extracted from the one studied. The boundary conditions of the simply supported shell are $N_x = M_x = v = w = 0$ for $x = 0$ and $x = L$, where N_x is the axial force and M_x is the bending moment per unit length. In particular, a symmetric system with respect to the angular coordinate $\theta = 0$ is assumed. Therefore, symmetric and antisymmetric modes with respect to this axis will be considered. The symmetric modes are expanded as

$$\begin{Bmatrix} u \\ v \\ w \end{Bmatrix}_S = \sum_{n=0}^{\infty} \sum_{m=1}^{\infty} \sum_{j=1}^{3} a_{nmj} \begin{Bmatrix} A_{nmj} & \cos(n\theta)\cos(m\pi x/L) \\ B_{nmj} & \sin(n\theta)\sin(m\pi x/L) \\ & \cos(n\theta)\sin(m\pi x/L) \end{Bmatrix}, \tag{1}$$

where a_{nmj} are the unknown coefficients involved in the mode expansion, A_{nmj} and B_{nmj} are the mode shape coefficients†, n, m and j indicate the number of circumferential waves, the number of axial half-waves and the mode number, respectively. In particular, the mode number $j = 1, 2, 3$ denotes modes with prevalent radial, angular and axial displacements, respectively. In fact, it is well known that the frequency equation of a simply supported shell is given by the following bi-cubic equation:

$$\Omega_{nmj}^6 - K_2\Omega_{nmj}^4 + K_1\Omega_{nmj}^2 - K_0 = 0 \tag{2}$$

which has three roots Ω_{nmj} for any given values of n and m; these roots correspond to $j = 1, 2, 3$. The coefficients K_0, K_1 and K_2 are given in the Appendix for the Flügge theory of shells and depend on the values of n and m. In equation (2), Ω_{nmj} is the frequency parameter, defined as

$$\Omega_{nmj}^2 = \omega_{nmj}^2 R^2 \rho_S (1 - \nu^2)/E, \tag{3}$$

† The normalization of the radial displacement to 1 gives a very high value, theoretically ∞, to B_{nmj} for the axisymmetric mode ($n = 0$) with prevalent angular displacement. In the numerical implementation, it is sufficient to use a large value.

where ω_{nmj} is the corresponding circular frequency, ρ_S is the shell mass density, E is Young's modulus and ν is the Poisson ratio. The mode shape coefficients A_{nmj} and B_{nmj} are computed by a linear system that is reported in the Appendix for the Flügge theory of shells. The antisymmetric modes with respect to $\theta = 0$ are expanded as

$$\begin{Bmatrix} u \\ v \\ w \end{Bmatrix}_A = \sum_{n=1}^{\infty} \sum_{m=1}^{\infty} \sum_{j=1}^{3} b_{nmj} \begin{Bmatrix} A_{nmj} & \sin(n\theta)\cos(m\pi x/L) \\ B_{nmj} & \cos(n\theta)\sin(m\pi x/L) \\ & \sin(n\theta)\sin(m\pi x/L) \end{Bmatrix}. \tag{4}$$

In the case that the system loses its symmetry with respect to $\theta = 0$, the following mode expansion must be considered:

$$\begin{Bmatrix} u \\ v \\ w \end{Bmatrix} = \begin{Bmatrix} u \\ v \\ w \end{Bmatrix}_S + \begin{Bmatrix} u \\ v \\ w \end{Bmatrix}_A. \tag{5}$$

The reference kinetic energy T_S^* of the shell, in the general case of expansion (5), is given by

$$\begin{aligned} T_S^* &= \tfrac{1}{2}\rho_S h \int_0^{2\pi}\int_0^L (u^2 + v^2 + w^2)\,\mathrm{d}x\,R\,\mathrm{d}\theta \\ &= \tfrac{1}{2}\rho_S h R\pi L \Bigg[\sum_{m=1}^{\infty}\sum_{j=1}^{3} a_{0mj}^2(1 + A_{0mj}^2 + B_{0mj}^2) \\ &\quad + \tfrac{1}{2}\sum_{n=1}^{\infty}\sum_{m=1}^{\infty}\sum_{j=1}^{3} (a_{nmj}^2 + b_{nmj}^2)(1 + A_{nmj}^2 + B_{nmj}^2)\Bigg]. \end{aligned} \tag{6}$$

The use of admissible functions that are the natural modes of a less-constrained problem, allows an interesting simplification, as observed by Amabili & Garziera (1999). In fact, the maximum potential energy V_S of the shell can be obtained as the multiplication of the reference kinetic energy of a natural mode in the less-constrained problem by the corresponding eigenvalue ω_{nmj}^2 (the squared circular frequency) of the shell and by the coefficients a_{nmj} or b_{nmj}, and then adding all the products. The result is

$$\begin{aligned} V_S = \tfrac{1}{2}\rho_S h R\pi L \Bigg[&\sum_{m=1}^{\infty}\sum_{j=1}^{3} a_{0mj}^2\omega_{0mj}^2(1 + A_{0mj}^2 + B_{0mj}^2) + \tfrac{1}{2}\sum_{n=1}^{\infty}\sum_{m=1}^{\infty}\sum_{j=1}^{3} \omega_{nmj}^2 \\ &\times (a_{nmj}^2 + b_{nmj}^2)(1 + A_{nmj}^2 + B_{nmj}^2)\Bigg]. \end{aligned} \tag{7}$$

In equation (7), the orthogonality of the eigenfunctions of the less-constrained problem has been used.

The maximum potential energy $V_{\tilde{k}}$ stored by the elastic distributed springs, which simulate the flexible axial translational constraint at $x = 0$, L, is given by

$$V_{\tilde{k}} = \tfrac{1}{2}\int_0^{2\pi} \tilde{k}(\theta)\,u^2(0,\theta)\,R\,\mathrm{d}\theta + \tfrac{1}{2}\int_0^{2\pi} \tilde{k}(\theta)\,u^2(L,\theta)R\,\mathrm{d}\theta. \tag{8}$$

In equation (8) $\tilde{k}(\theta)$ is the nonuniform spring stiffness (N/m^2) that is assumed to be the same at $x = 0$ and L. For simplicity, $\tilde{k}(\theta)$ is assumed to be symmetric with respect to $\theta = 0$, and it can be expanded into the following cosine series:

$$\tilde{k}(\theta) = \sum_{k=0}^{\infty} \tilde{k}_k \cos(k\theta). \tag{9}$$

From now on, the system is assumed to be symmetric with respect to $\theta = 0$. This hypothesis simplifies the calculations, without loss of generality, and can easily be removed. For symmetric modes, the substitution of equations (1) and (9) into equation (8) gives

$$V_{\tilde{k}} = \tfrac{1}{2} R \sum_{n,s=0}^{\infty} \sum_{m,i=1}^{\infty} \sum_{j,\tilde{j}=1}^{3} \sum_{k=0}^{\infty} \psi_{nsk} \tilde{k}_k a_{nmj} a_{si\tilde{j}} A_{nmj} A_{si\tilde{j}} [1 + (-1)^m (-1)^i], \tag{10}$$

where

$$\psi_{nsk} = \int_0^{2\pi} \cos(n\theta)\cos(s\theta)\cos(k\theta)\,\mathrm{d}\theta = \begin{cases} 2\pi & \text{if } n = s = k = 0, \\ \pi & \text{if } k = 0 \text{ and } n = s \neq 0, \\ \pi & \text{if } n = 0 \text{ and } s = k \neq 0, \\ \pi & \text{if } s = 0 \text{ and } n = k \neq 0, \\ \pi/2 & \text{if } k = n + s \text{ and } n \neq 0 \text{ and } s \neq 0, \\ \pi/2 & \text{if } s = n + k \text{ and } k \neq 0 \text{ and } n \neq 0, \\ \pi/2 & \text{if } n = s + k \text{ and } k \neq 0 \text{ and } s \neq 0, \\ 0 & \text{otherwise.} \end{cases} \tag{11}$$

For antisymmetric modes, the substitution of equations (2) and (9) into equation (8) gives

$$V_{\tilde{k}} = \tfrac{1}{2} R \sum_{n,s=1}^{\infty} \sum_{m,i=1}^{\infty} \sum_{j,\tilde{j}=1}^{3} \sum_{k=0}^{\infty} \varphi_{nsk} \tilde{k}_k b_{nmj} b_{si\tilde{j}} A_{nmj} A_{si\tilde{j}} [1 + (-1)^m (-1)^i], \tag{12}$$

where

$$\varphi_{nsk} = \int_0^{2\pi} \sin(n\theta)\sin(s\theta)\cos(k\theta)\,\mathrm{d}\theta = \begin{cases} \pi & \text{if } k = 0 \text{ and } n = s, \\ -\pi/2 & \text{if } k = n + s, \\ \pi/2 & \text{if } s = n + k \text{ and } k \neq 0, \\ \pi/2 & \text{if } n = s + k \text{ and } k \neq 0, \\ 0 & \text{otherwise.} \end{cases} \tag{13}$$

The maximum potential energy V_c stored by the elastic distributed rotational springs, that simulate the flexible rotational constraint at $x = 0, L$, is given by

$$V_c = \tfrac{1}{2} \int_0^{2\pi} c(\theta) \left[\frac{\partial w}{\partial x}(0, \theta) \right]^2 R\,\mathrm{d}\theta + \tfrac{1}{2} \int_0^{2\pi} c(\theta) \left[\frac{\partial w}{\partial x}(L, \theta) \right]^2 R\,\mathrm{d}\theta. \tag{14}$$

In equation (14) $c(\theta)$ is the nonuniform rotational spring stiffness (N) that is assumed to be the same at $x = 0$ and L. Similarly to $\tilde{k}(\theta)$, $c(\theta)$ is assumed to be symmetric with respect to $\theta = 0$; it can be expanded into the following cosine series:

$$c(\theta) = \sum_{k=0}^{\infty} c_k \cos(k\theta). \tag{15}$$

For symmetric modes, substitution of equations (1) and (15) into equation (14) gives

$$V_c = \tfrac{1}{2} R \sum_{n,s=0}^{\infty} \sum_{m,i=1}^{\infty} \sum_{j,\tilde{j}=1}^{3} \sum_{k=0}^{\infty} \psi_{nsk} c_k a_{nmj} a_{si\tilde{j}} (mi\pi^2/L^2) [1 + (-1)^m (-1)^i]. \tag{16}$$

Similarly, for antisymmetric modes

$$V_c = \tfrac{1}{2} R \sum_{n,s=1}^{\infty} \sum_{m,i=1}^{\infty} \sum_{j,\tilde{j}=1}^{3} \sum_{k=0}^{\infty} \varphi_{nsk} c_k b_{nmj} b_{si\tilde{j}} (mi\pi^2/L^2) [1 + (-1)^m (-1)^i]. \tag{17}$$

It is interesting to note that a fully clamped shell is obtained by setting a uniform and very high value to the stiffnesses of the translational and rotational springs $\tilde{k}$ and c. The values of the spring stiffnesses simulating a clamped shell can be obtained by trial and error, or by evaluating the edge stiffness of the shell. In fact, it was found that the natural frequencies of the system converge asymptotically to those of a clamped shell when $\tilde{k}$ and c become very large.

A second observation concerns shells used in engineering applications. In practice, it can be easier to make a rigid rotational constraint (corresponding to $c \to \infty$) than a rigid axial constraint ($\tilde{k} \to \infty$). As a consequence that in many cases the influence of the axial constraint on the natural frequencies of shells is very important, one should specify if a clamped shell is assumed only constrained with respect to rotation or if it is a fully clamped shell with constrained axial displacement u at the shell ends.

3. COMPLICATING EFFECTS

An important advantage of the present method is that additional complicating effects can be included into the original problem, by adding energy terms without any complication in the approach. In particular, the effects of a contained inviscid fluid, of a nonuniform elastic bed and of an added mass are considered here as examples. Additional intermediate constraints to shell motion in the radial direction can be obtained by conveniently setting the stiffness of the elastic bed; intermediate constraints in other directions and rotational constraints can be treated similarly.

The present approach can easily be extended to shells with nonuniform thickness in the circumferential and axial directions. The natural modes of the simply supported shell of uniform thickness equal to the minimum thickness of the nonuniform shell can be used as the base, and all the energies must be calculated by considering the thickness h as a function of the coordinates θ and x. However, the maximum potential energy of the shell cannot be computed by using equation (7) anymore, as observed by Amabili & Garziera (1999) in the case of beams. In this case the maximum potential energy of the shell must be evaluated by using the expression deriving form the shell theory used, e.g. Cheng & Nicolas (1992). Cheung & Zhou (1999) applied a new set of beam functions to study vibrations of tapered rectangular plates; similar functions could be also applied for shells with nonuniform thickness.

3.1. Contained Inviscid Fluid

The shell is considered completely filled with an inviscid and incompressible fluid. The ends of the shell are assumed to be open. The hydrostatic pressure effect is neglected in the following study. For an incompressible and inviscid fluid, its deformation potential satisfies the Laplace equation

$$\nabla^2 \phi(x, \theta, r) = 0. \tag{18}$$

The deformation potential ϕ is related to the velocity potential $\tilde{\phi}$ by

$$\tilde{\phi}(x, \theta, r, t) = \mathrm{i}\omega\phi \mathrm{e}^{\mathrm{i}\omega t}, \tag{19}$$

which is assumed to be harmonic. The velocity of the fluid $\mathbf{v}$ is related to $\tilde{\phi}$ by $\mathbf{v} = \text{grad}\,\tilde{\phi}$.

The Laplace equation (18) is solved with the boundary conditions

$$\phi = 0 \quad \text{at} \quad x = 0, L \quad \text{and} \quad (\partial\phi/\partial r)_{r=R} = -w, \tag{20, 21}$$

and ϕ must be regular in the fluid domain. Equation (20) states that the shell ends are open and equation (21) ensures a contact between the shell wall and the fluid. Solution of Laplace equation satisfying equation (20) and regularity is (e.g. Amabili 1999)

$$\phi = \sum_{m=1}^{\infty}\sum_{j=1}^{3} \alpha_{0mj} \mathrm{I}_0(m\pi r/L)\sin(m\pi x/L) + \sum_{n=1}^{\infty}\sum_{m=1}^{\infty}\sum_{j=1}^{3} [\alpha_{nmj}\cos(n\theta) + \beta_{nmj}\sin(n\theta)]\,\mathrm{I}_n(m\pi r/L)\sin(m\pi x/L), \tag{22}$$

where I_n is the modified Bessel function of order n. Applying condition (21), one obtains

$$\alpha_{0mj} = -\frac{a_{0mj}}{(m\pi/L)\mathrm{I}_0'(m\pi R/L)}, \tag{23}$$

$$\alpha_{nmj} = -\frac{a_{nmj}}{(m\pi/L)\,\mathrm{I}_n'(m\pi R/L)}, \tag{24}$$

$$\beta_{nmj} = -\frac{b_{nmj}}{(m\pi/L)\mathrm{I}_n'(m\pi R/L)}, \tag{25}$$

where the prime indicates the derivative with respect to the argument.

The reference kinetic energy of the contained fluid, by using Green's theorem (e.g. Amabili 1997), is

$$\begin{aligned} T_F^* &= \frac{1}{2}\rho_F \int_0^L\int_0^{2\pi} \left(\phi\frac{\partial\phi}{\partial r}\right)_{r=R} \mathrm{d}x R\,\mathrm{d}\theta = -\frac{1}{2}\rho_F R \int_0^L\int_0^{2\pi} (\phi)_{r=R}\, w\,\mathrm{d}x\,\mathrm{d}\theta \\ &= \frac{1}{2}\rho_F R\frac{L}{2}\pi\left[2\sum_{m=1}^{\infty}\sum_{j=1}^{3} a_{0mj}^2 \frac{\mathrm{I}_0(m\pi R/L)}{(m\pi/L)I_0'(m\pi R/L)} + \sum_{n=1}^{\infty}\sum_{m=1}^{\infty}\sum_{j=1}^{3}(a_{nmj}^2 + b_{nmj}^2)\frac{\mathrm{I}_n(m\pi R/L)}{(m\pi/L)\,\mathrm{I}_n'(m\pi R/L)}\right], \end{aligned} \tag{26}$$

where ρ_F is the mass density of the fluid.

3.2. Elastic Bed

The maximum potential energy V_B stored by an elastic bed composed of radial elastic springs of stiffness $\tilde{b}(x, \theta)$ is given by

$$V_B = \tfrac{1}{2}\int_0^{2\pi}\int_0^L \tilde{b} w^2\,\mathrm{d}x R\,\mathrm{d}\theta, \tag{27}$$

where the stiffness $\tilde{b}(x, \theta)$ of the bed ($\mathrm{N/m^3}$) is assumed to be symmetric with respect to $\theta = 0$ and to $x = L/2$. For the symmetry hypothesis, $\tilde{b}(x, \theta)$ can be expanded into the following series:

$$\tilde{b}(x, \theta) = \sum_{k=0}^{\infty}\sum_{l=0}^{\infty} \tilde{b}_{kl}\cos(k\theta)\cos(2l\pi x/L). \tag{28}$$

For symmetric modes one obtains

$$V_B = \tfrac{1}{2} R \sum_{n,s=0}^{\infty} \sum_{m,i=1}^{\infty} \sum_{j,\tilde{j}=1}^{3} \sum_{k,l=0}^{\infty} \psi_{nsk} \mu_{mil} \tilde{b}_{kl} a_{nmj} a_{si\tilde{j}}, \tag{29}$$

where

$$\mu_{mil} = \int_0^L \sin(m\pi x/L) \sin(i\pi x/L) \cos(2l\pi x/L)\, \mathrm{d}x = \begin{cases} L/2 & \text{if } l = 0 \text{ and } i = m, \\ 0 & \text{if } l = 0 \text{ and } i \neq m, \\ L/4 & \text{if } i \pm 2l - m = 0 \text{ and } l \neq 0, \\ -L/4 & \text{if } i \pm 2l + m = 0 \text{ and } l \neq 0, \\ 0 & \text{otherwise.} \end{cases} \tag{30}$$

Similarly, for antisymmetric modes

$$V_B = \tfrac{1}{2} R \sum_{n,s=1}^{\infty} \sum_{m,i=1}^{\infty} \sum_{j,\tilde{j}=1}^{3} \sum_{k,l=0}^{\infty} \varphi_{nsk} \mu_{mil} \tilde{b}_{kl} b_{nmj} b_{si\tilde{j}}. \tag{31}$$

3.3. Added Mass

A lumped mass M (kg) at $x = x^*$, $\theta = \theta^*$ is considered. The reference kinetic energy of the added mass is given by

$$T_M^* = \tfrac{1}{2} M [u^2(x^*, \theta^*) + v^2(x^*, \theta^*) + w^2(x^*, \theta^*)]. \tag{32}$$

As usual, a symmetric distribution of added masses with respect to $\theta = 0$ is assumed; therefore, in the case of one mass only, $\theta^* = \pi$ is assumed. For symmetric modes one obtains

$$T_M^* = \tfrac{1}{2} M \sum_{n,s=0}^{\infty} \sum_{m,i=1}^{\infty} \sum_{j,\tilde{j}=1}^{3} a_{nmj} a_{si\tilde{j}} (-1)^n (-1)^s [\sin(m\pi x^*/L) \sin(i\pi x^*/L) + A_{nmj} A_{si\tilde{j}} \cos(m\pi x^*/L) \cos(i\pi x^*/L)]. \tag{33}$$

For antisymmetric modes one obtains

$$T_M^* = \tfrac{1}{2} M \sum_{n,s=1}^{\infty} \sum_{m,i=1}^{\infty} \sum_{j,\tilde{j}=1}^{3} b_{nmj} b_{si\tilde{j}} (-1)^n (-1)^s B_{nmj} B_{si\tilde{j}} \sin(m\pi x^*/L) \sin(i\pi x^*/L); \tag{34}$$

this means that an added mass located at $\theta^* = \pi$ only affects the tangential displacement of antisymmetric modes. The effect of a distributed mass is obtained as a natural extension.

4. EIGENVALUE PROBLEM

The Rayleigh quotient for the problem studied is given by

$$\Omega^2 = \frac{V_S + V_{\tilde{k}} + V_c + V_B}{T_S^* + T_F^* + T_M^*}, \tag{35}$$

Ω being the circular frequency (rad/s) of the system. Only a finite number of modes in the Rayleigh-Ritz expansion are retained. The matrix $\mathbf{q}$ of the Ritz coefficients is introduced,

$$q_{nmj} = \begin{cases} a_{nmj} & \text{for symmetric modes, } n = 0, \ldots, N-1;\ m = 1, \ldots, \tilde{N};\ j = 1,2,3, \\ b_{nmj} & \text{for antisymmetric modes, } n = 1, \ldots, N;\ m = 1, \ldots, \tilde{N};\ j = 1, 2, 3. \end{cases} \tag{36}$$

In equation (36) the expansion of symmetric and antisymmetric modes involves $3 \times N \times \tilde{N}$ terms; N and $\tilde{N}$ must be chosen large enough to give the required accuracy.

The reference kinetic energy of the shell, equation (6), can be written in the following vectorial notation:

$$T_S^* = \tfrac{1}{2}\,\rho_S h R (L/2)\,\mathbf{q}^{\mathrm{T}}\mathbf{M}_S\mathbf{q}, \tag{37}$$

where the matrix $\mathbf{M}_S$ is given by

$$(\mathbf{M}_S)_{nsmi\tilde{j}\tilde{j}} = \begin{cases} 2\pi\delta_{ns}\delta_{mi}\delta_{\tilde{j}\tilde{j}}(1 + A_{0mj}^2 + B_{0mj}^2) & \text{if } n = 0, \\ \pi\delta_{ns}\delta_{mi}\delta_{\tilde{j}\tilde{j}}(1 + A_{nmj}^2 + B_{nmj}^2) & \text{if } n > 0. \end{cases} \tag{38}$$

δ_{ns} is the Kronecker delta as well as δ_{mi} and $\delta_{\tilde{j}\tilde{j}}$; s, i and $\tilde{j}$ have the same range of values of n, m and j, respectively. The maximum potential energy of the shell, equation (7), can be written as

$$V_S = \tfrac{1}{2}\,\rho_s h R (L/2)\,\mathbf{q}^{\mathrm{T}}\mathbf{K}_S\mathbf{q}, \tag{39}$$

where the matrix $\mathbf{K}_S$ is given by

$$(\mathbf{K}_S)_{nsmi\tilde{j}\tilde{j}} = \begin{cases} 2\pi\delta_{ns}\delta_{mi}\delta_{\tilde{j}\tilde{j}}\omega_{nmj}^2(1 + A_{0mj}^2 + B_{0mj}^2) & \text{if } n = 0, \\ \pi\delta_{ns}\delta_{mi}\delta_{\tilde{j}\tilde{j}}\omega_{nmj}^2(1 + A_{nmj}^2 + B_{nmj}^2) & \text{if } n > 0. \end{cases} \tag{40}$$

The maximum potential energy stored by the elastic distributed springs, by using equations (10) and (12), is

$$V_{\tilde{k}} = \tfrac{1}{2}\,R\mathbf{q}^{\mathrm{T}}\mathbf{K}_{\tilde{k}}\mathbf{q}, \tag{41}$$

where the matrix $\mathbf{K}_{\tilde{k}}$ is

$$(\mathbf{K}_{\tilde{k}})_{nsmi\tilde{j}\tilde{j}} = \sum_{k=0}^{\infty} \psi_{nsk}\tilde{k}_k A_{nmj} A_{si\tilde{j}}[1 + (-1)^m(-1)^i] \quad \text{for symmetric modes,} \tag{42}$$

$$(\mathbf{K}_{\tilde{k}})_{nsmi\tilde{j}\tilde{j}} = \sum_{k=0}^{\infty} \varphi_{nsk}\tilde{k}_k A_{nmj} A_{si\tilde{j}}[1 + (-1)^m(-1)^i] \quad \text{for antisymmetric modes.} \tag{43}$$

In equations (42) and (43) the sums on k are stopped, in numerical computations, at an integer value large enough to give the required accuracy. The maximum potential energy stored by the elastic, rotational springs, obtained by equations (16) and (17), is

$$V_c = \tfrac{1}{2} R\mathbf{q}^{\mathrm{T}}\mathbf{K}_c\mathbf{q}, \tag{44}$$

where the matrix $\mathbf{K}_c$ is given by

$$(\mathbf{K}_c)_{nsmi\tilde{j}\tilde{j}} = \sum_{k=0}^{\infty} \psi_{nsk} c_k (mi\pi^2/L^2)[1 + (-1)^m(-1)^i] \quad \text{for symmetric modes,} \tag{45}$$

$$(\mathbf{K}_c)_{nsmi\tilde{j}\tilde{j}} = \sum_{k=0}^{\infty} \varphi_{nsk} c_k (mi\pi^2/L^2)[1 + (-1)^m(-1)^i] \quad \text{for antisymmetric modes.} \tag{46}$$

The reference kinetic energy of the fluid contained into the shell, equation (26), can be written as

$$T_F^* = \tfrac{1}{2}\,\rho_F R (L/2)\,\mathbf{q}^{\mathrm{T}}\mathbf{M}_F\mathbf{q}, \tag{47}$$

where the matrix $\mathbf{M}_F$ is given by

$$(\mathbf{M}_F)_{nsmij\tilde{j}} = \begin{cases} 2\delta_{ns}\delta_{mi}\delta_{j\tilde{j}} \dfrac{\mathrm{I}_0(m\pi R/L)}{(m/L)\,\mathrm{I}'_0(m\pi R/L)} & \text{if } n = 0, \\ \delta_{ns}\delta_{mi}\delta_{j\tilde{j}} \dfrac{\mathrm{I}_n(m\pi R/L)}{(m/L)\,\mathrm{I}'_n(m\pi R/L)} & \text{if } n > 0. \end{cases} \tag{48}$$

The maximum potential energy stored by the elastic bed, obtained by equations (29) and (31), is

$$V_B = \tfrac{1}{2} R\mathbf{q}^{\mathrm{T}}\mathbf{K}_{\mathrm{B}}\mathbf{q}, \tag{49}$$

where the matrix $\mathbf{K}_B$ is given by

$$(\mathbf{K}_B)_{nsmij\tilde{j}} = \sum_{k=0}^{\infty}\sum_{l=0}^{\infty} \psi_{nsk}\mu_{mil}\tilde{b}_{kl} \quad \text{for symmetric modes,} \tag{50}$$

$$(\mathbf{K}_B)_{nsmij\tilde{j}} = \sum_{k=0}^{\infty}\sum_{l=0}^{\infty} \varphi_{nsk}\mu_{mil}\tilde{b}_{kl} \quad \text{for antisymmetric modes.} \tag{51}$$

The reference kinetic energy stored by the lumped added mass, obtained by equations (33) and (34), is

$$T^*_M = \tfrac{1}{2} M\mathbf{q}^{\mathrm{T}}\mathbf{M}_M\mathbf{q}, \tag{52}$$

where the matrix $\mathbf{M}_M$ for symmetric modes is given by

$$(\mathbf{M}_M)_{nsmij\tilde{j}} = (-1)^n(-1)^s[\sin(m\pi x^*/L)\sin(i\pi x^*/L) + A_{nmj}A_{si\tilde{j}}\cos(m\pi x^*/L)\cos(i\pi x^*/L)], \tag{53}$$

and for antisymmetric modes by

$$(\mathbf{M}_M)_{nsmij\tilde{j}} = (-1)^n(-1)^s B_{nmj}B_{si\tilde{j}}\sin(m\pi x^*/L)\sin(i\pi x^*/L). \tag{54}$$

The problem is solved minimizing the Rayleigh quotient, equation (35); this operation gives the following Galerkin equation:

$$[\rho_S h(L/2)\mathbf{K}_S + \mathbf{K}_{\tilde{k}} + \mathbf{K}_c + \mathbf{K}_B]\mathbf{q} - \Omega^2[\rho_S h(L/2)\mathbf{M}_S + \rho_F(L/2)\mathbf{M}_F + (M/R)\mathbf{M}_M]\,\mathbf{q} = 0. \tag{55}$$

5. NUMERICAL IMPLEMENTATION

The solution of the problem is obtained with a self-made code written in C language. The matrices with six indices given in Section 4 are transformed in matrices with two indices (plane matrices); this transformation is explained in Figure 2. The solution of the generalized eigenvalue problem for real symmetric matrices given in equation (55) is obtained by using a general iterative method based on a modified routine of the *Lapack* package (NAG).

The computational load increases by N^4 if all the natural frequencies available with the used expansion are required, where N indicates the number of axial or circumferential modes retained in the expansion. From the algorithmic point of view, this problem is easily modularized and the matrices associated with the complicating effects are separately built.

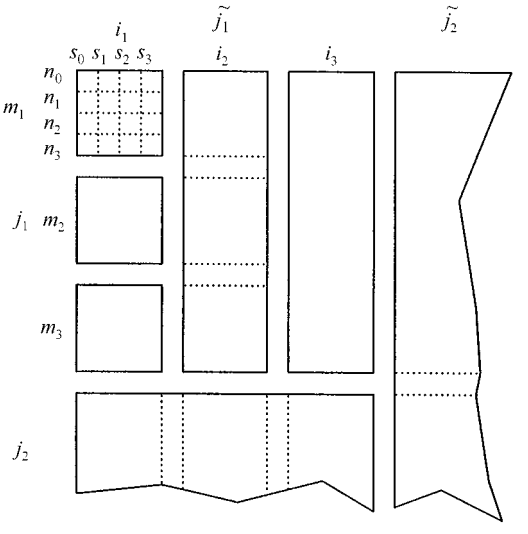

Figure 2. Reduction of the six-index matrix to a two-index matrix.

6. NUMERICAL RESULTS

Numerical results are obtained (i) to validate the method and to show its accuracy; (ii) to study riveted shells; (iii) to study shells embedded on an elastic bed having partial extension in longitudinal and angular directions including the case of shells with intermediate constraints; (iv) to study water-filled, riveted shell with partial elastic bed. It must be observed that the effect of damping due to friction at the bolted or riveted joint (Shin *et al.* 1991; Jézéquel 1983) and all other nonlinear effects are neglected.

6.1. Validation of the Method

The present method and the code developed have been tested with some cases already studied in the literature. Initially a fully clamped shell, i.e. $u = v = w = \partial w/\partial x = 0$ for $x = 0$ and L, previously studied by Koval & Cranch (1962) and also discussed by Leissa (1970) has been considered. The same case was also studied by Cheng & Nicolas (1992) and by Vronay & Smith (1970) for modes with $n \leq 5$. It has the following characteristics: $R = 0{\cdot}0762$ m, $L = 0{\cdot}3048$ m, $h = 0{\cdot}000254$ m, $E = 204 \times 10^9$ Pa, $\rho = 7836{\cdot}6$ kg/m^3 and $\nu = 0{\cdot}3$. The results obtained are given in Tables 1 and 2 and are in good agreement with those reported by Koval & Cranch (1962), by Cheng & Nicolas (1992) and by Vronay & Smith (1970). The theoretical results of Koval & Cranch (1962) were obtained with Donnell's shell theory by using clamped–clamped beam functions.

In the present approach, 3×35 modes are used in the Ritz expansion for any given number of circumferential waves. $\tilde{k} = 10^9$ N/m^2 and $c = 10^8$ N are used to simulate rigid translational and rotational artificial springs; these values have been found by trial and error, and incrementing these values does not change the results. It is very important to note that the effect of the edge axial constraint is fundamental to calculate correctly the natural frequencies of the system. Therefore, it is important to retain in the expansion of the shell displacement not only flexural modes ($j = 1$) but also modes with prevalent axial and torsional displacements ($j = 2$, 3). In Table 1, both natural frequencies computed with 3×35 modes and 3×50 modes in the Ritz expansion are given to show the convergence.

TABLE 1

Natural frequencies of a circular cylindrical shell clamped at the ends; n is the number of circumferential waves. Only modes with one axial half-wave are considered. In the second column, results in parentheses are computed with 3×50 modes in the Ritz expansion, the others with 3×35 modes

n	Present study	Theory from Koval & Cranch (1962)	Experiments from Koval & Cranch (1962)
3	1132 (1124)	1176	1025
4	761 (755)	783	700
5	579 (575)	597	522
6	534 (531)	552	525
7	590 (589)	611	592
8	713 (713)	736	720

TABLE 2

Natural frequencies of a circular cylindrical shell clamped at the ends; results in round parentheses are from Cheng & Nicolas (1992) and in square parentheses from Vronay & Smith (1970)

Number of axial half-waves	Number of circumferential waves 3	4	5
1	1132 (1163) [1154]	761 (769) [765]	579 (581) [581]
2	2623 (2659) [2536]	1820 (1832) [1752]	1335 (1335) [1287]

In particular, 3×35 modes give a good approximation in this case. A deeper investigation of the degree of convergence is deferred to Section 6.2.

A second case used for comparison is a simply supported shell, empty or water-filled, with a lumped lead mass of 96·7 g attached. The shell has the following characteristics: $R = 0{\cdot}175$ m, $L = 0{\cdot}664$ m, $h = 0{\cdot}001$ m, $E = 206 \times 10^9$ Pa, $\rho = 7700$ kg/m^3 $\rho_F = 1000$ kg/m^3 and $v = 0{\cdot}3$. The first three mode shapes and natural frequencies of the empty shell are shown in Figure 3 and compared with theoretical and experimental data reported by Amabili (1996). Theoretical results of Amabili (1996) were obtained by using the receptance method. Similarly, Figure 4 shows results for the water-filled shell. The agreement of results is remarkable for both the empty and water-filled shell. Results were obtained with $3 \times 30 \times 30$ modes in the expansion.

6.2. RIVETED SHELLS

The same shell previously studied by Amabili (1996) and also used in the previous section is considered here, with the only difference that $\rho = 7800$ kg/m^3; $3 \times 32 \times 20$ modes are considered in the expansion, where 31 is the maximum number of circumferential waves and 20 is the maximum number of axial half-waves. Natural modes of this riveted shell are studied by imposing N equispaced clamped arcs of angular amplitude of $3{\cdot}5^\circ$ at each shell end. The rivets are symmetrically distributed with respect to the origin $\theta = 0$ and away from this point (see Figure 5); both slope in the axial direction and axial displacements are restrained at the rivet location by using springs of very high stiffness, simulating rigid constraints. Outside these clamped arcs the shell is simply supported. This hypothesis is

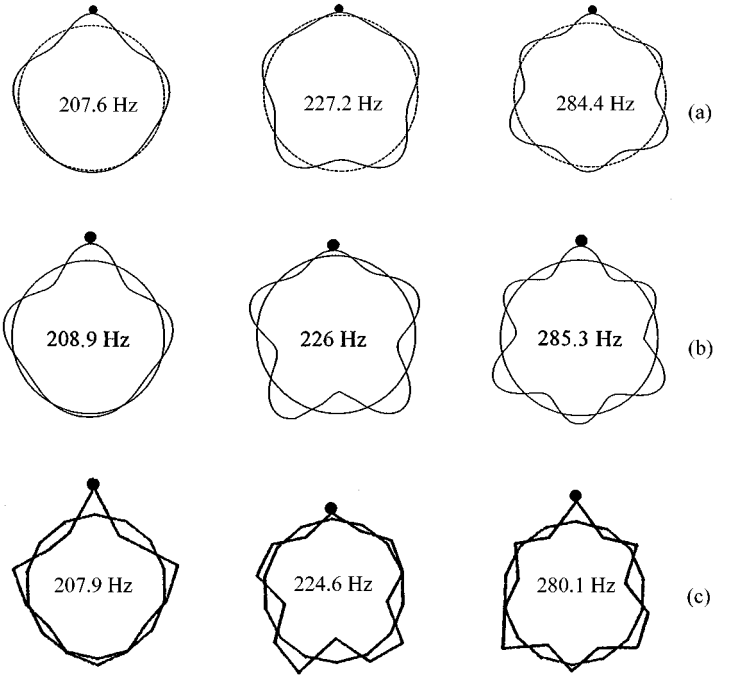

Figure 3. First three mode shapes and natural frequencies of the empty shell: (a) computed modes; (b) modes computed by Amabili (1996); (c) experimental modes (Amabili 1996).

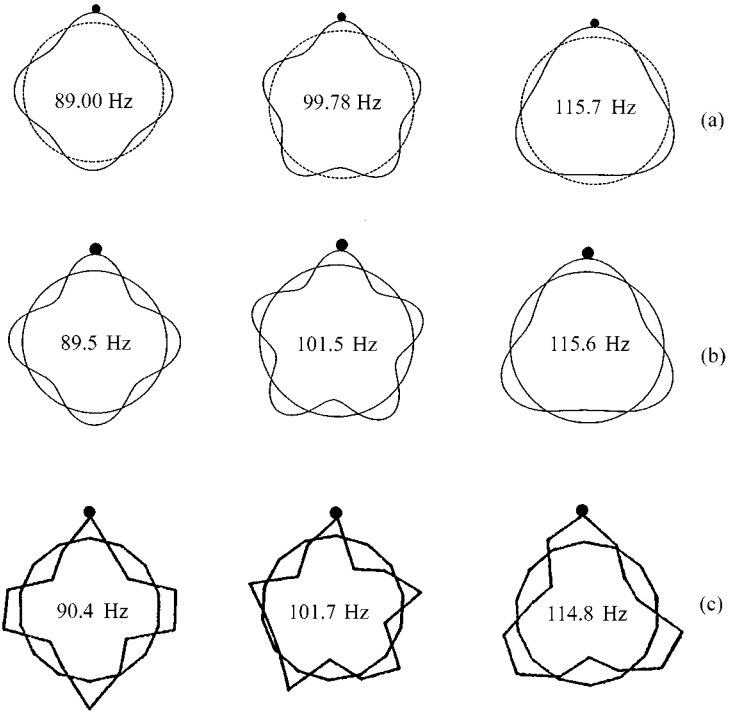

Figure 4. First three mode shapes and natural frequencies of the water-filled shell: (a) computed modes; (b) modes computed by Amabili (1996); (c) experimental modes (Amabili 1996).

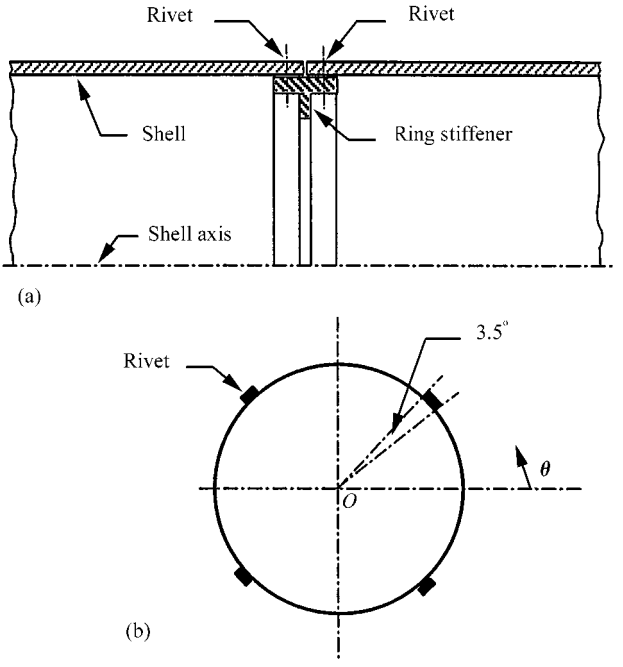

Figure 5. Drawing of riveted shell: (a) shell riveted at ring-stiffener location; (b) equispaced rivets, symmetrically placed with respect to $\theta = 0$ and away from this point.

good enough for inward displacement; in fact, in engineering applications, rivets are often positioned at the ring-stiffeners (see Figure 5) that make the shell cross-section almost undeformable at these axial locations. The outward displacement is not restrained in a similar way, making the actual problem nonlinear. Here, the problem with restrained outward displacement of the shell between the rivets is assumed for simplicity; practically it is realized when the shell is glued to the stiffener, e.g. to avoid fluid leakage.

Natural frequencies of symmetric and antisymmetric modes versus the number N of rivets is given in Figure 6. It is very interesting to observe that an increment of the frequency does not necessarily follow an increment of the number of rivets. In fact, when the number of rivets is equal to the number of nodal diameters of the mode considered, there is a local minimum of the natural frequency. A decrement of the number of rivets from this particular value is associated with a movement of the rivets from the nodes and with an increment of the natural frequency. In Figure 6 extreme values, obtained with no rivets (simply supported shell) and an infinite number of rivets (clamped shell) are reported.

The convergence of the method with the number of circumferential and axial modes used in the expansion is shown in Figure 7 for a shell with four rivets. It shows that 3×25 modes in both circumferential and axial directions give a good accuracy. A discussion on the convergence of the method can be found in Amabili and Garziera (1999).

Figures 8 and 9 show the first four symmetric and antisymmetric modes, respectively, for the shell fixed with four rivets. Natural frequencies are given in the captions and are comprised between those of the simply supported and those of the clamped shell. The fundamental mode with four rivets is the first antisymmetric mode. The figures show only the radial displacement. The shell slope in the axial direction is zero at the rivets, as shown in Figures 8 and 9.

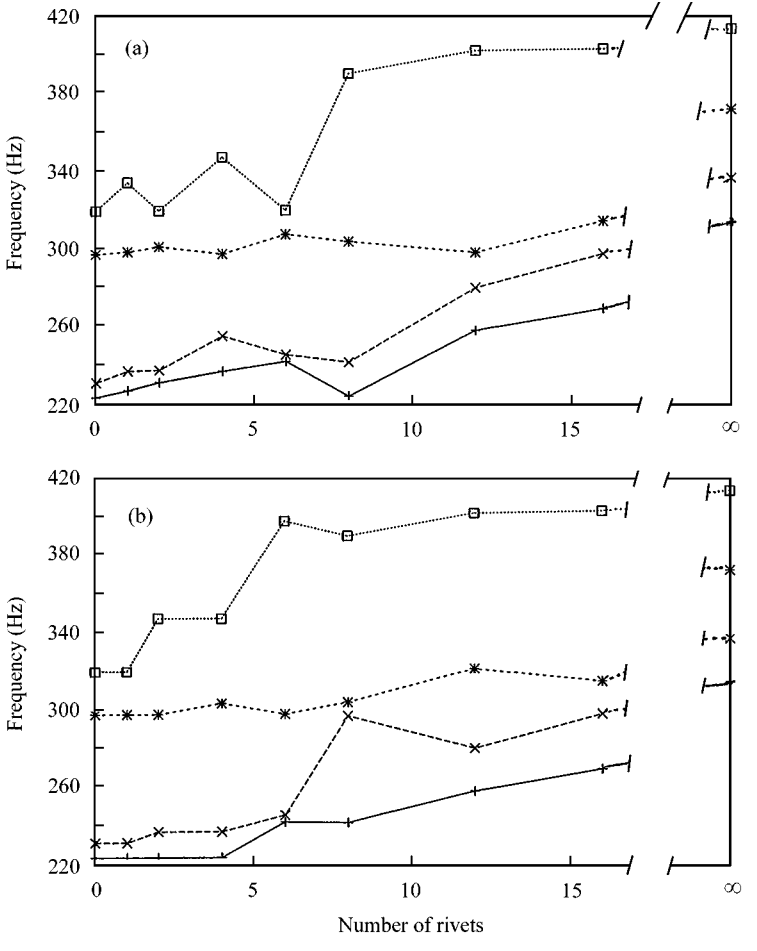

Figure 6. First four natural frequencies of the empty shell versus the number of rivets (clamped arcs): (a) symmetric modes; (b) antisymmetric modes.

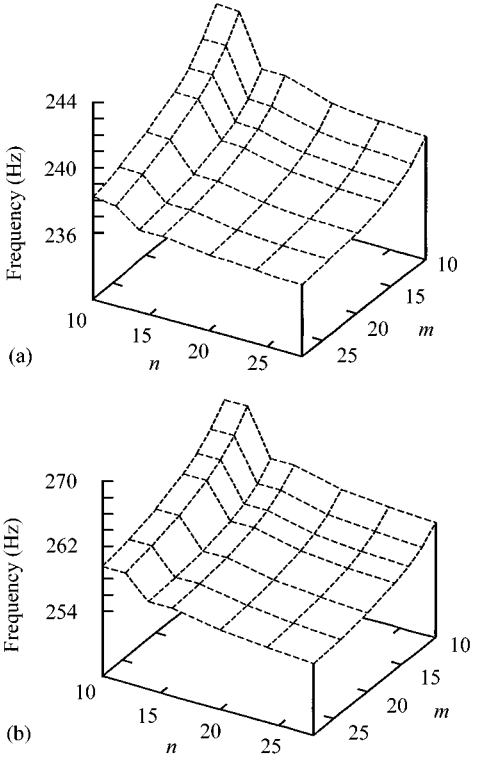

Figure 7. Computed natural frequencies versus the number of circumferential (n) and axial (m) modes considered in the expansion for any $j = 1, 2, 3$: (a) first symmetric mode; (b) second symmetric mode.

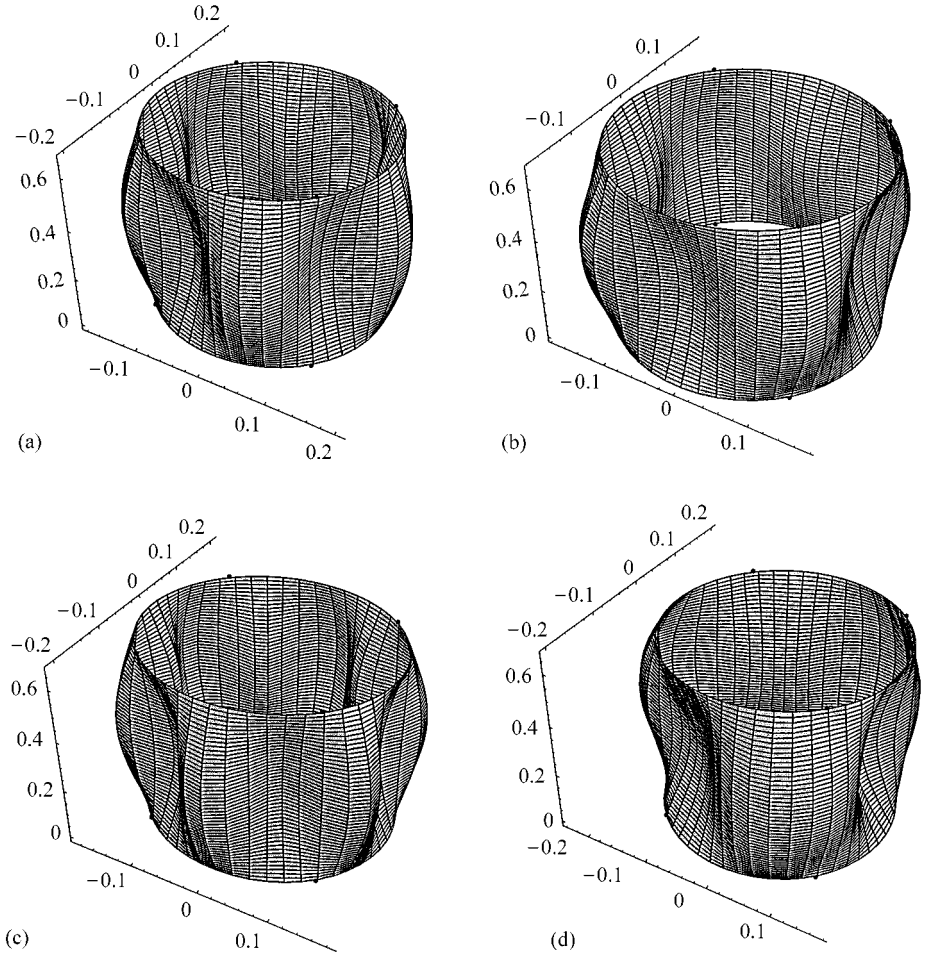

Figure 8. Symmetric modes of the empty shell with four rivets: (a) first mode, 238 Hz; (b) second mode, 256 Hz; (c) third mode, 298 Hz; (d) fourth mode, 348 Hz.

The effect of the stiffness of the artificial translational and rotational springs at the rivet locations is investigated in Figure 10, assuming $\tilde{k}(\theta) = c(\theta)$. In this case, the rotational springs give an horizontal asymptote for a value of $c(\theta)$ lower than the one necessary for the translational springs to reach an horizontal line. The figure shows that an increment of the stiffness of the translational springs superior to 10^9 N/m^2 does not give any significant increase to the frequency of the first symmetric mode; this value is large enough to simulate a rigid constraint with a good accuracy.

Figure 11 is analogous to Figure 6 but is relative to the water-filled shell. The effect of the contained water is that of reducing drastically the natural frequencies of the system. A second interesting phenomenon is that the mode order is changed by the added virtual mass. This is shown, e.g. by comparing Figures 6(a) and 11(a); in particular, the curve relative to the fourth mode in Figure 6(a) has almost the same shape as the curve for the third mode in Figure 11(a). These two curves correspond to modes with almost the same shape, even if their order is changed. A last interesting difference with respect to the empty shell is that a larger number of rivets (clamped arcs) is necessary to approximate a clamped

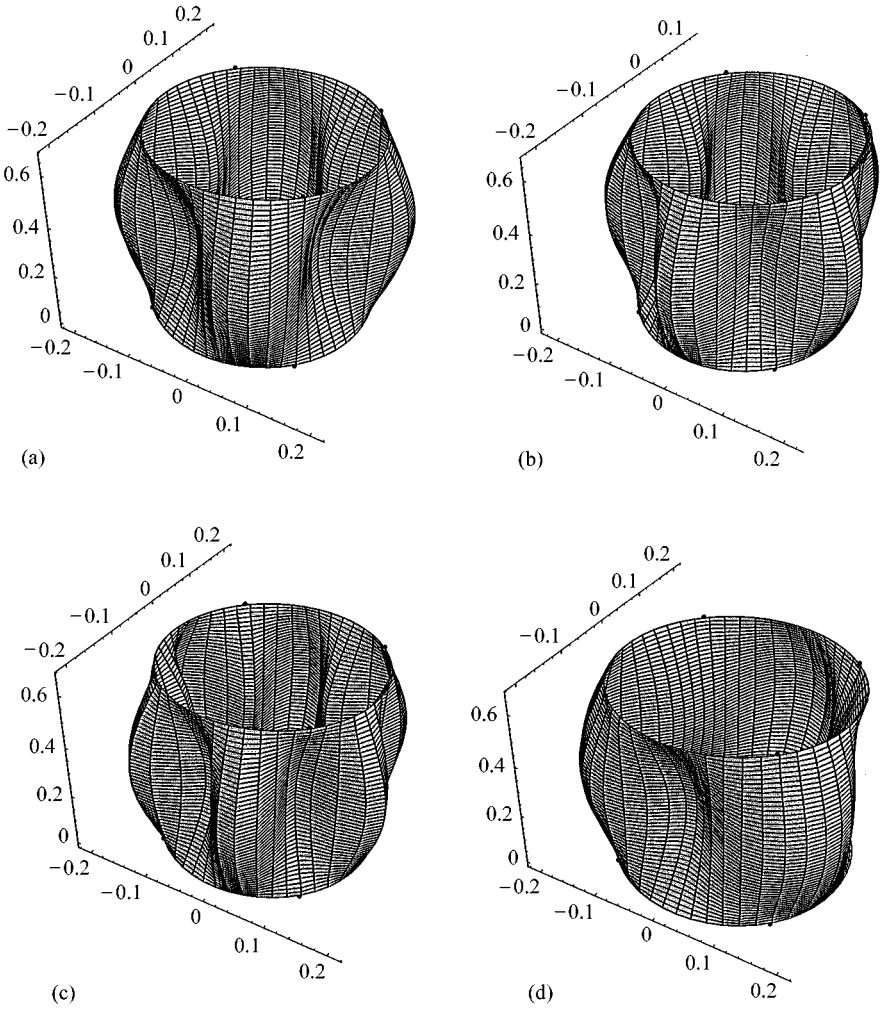

Figure 9. Antisymmetric modes of the empty shell with four rivets: (a) first mode, 224 Hz; (b) second mode, 237 Hz; (c) third mode, 304 Hz; (d) fourth mode, 348 Hz.

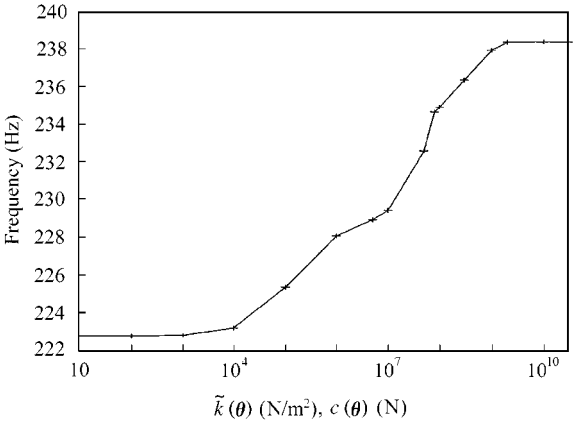

Figure 10. Natural frequency of the first symmetric mode of the empty shell with four rivets versus the rivet stiffness, assuming $\tilde{k}(\theta) = c(\theta)$.

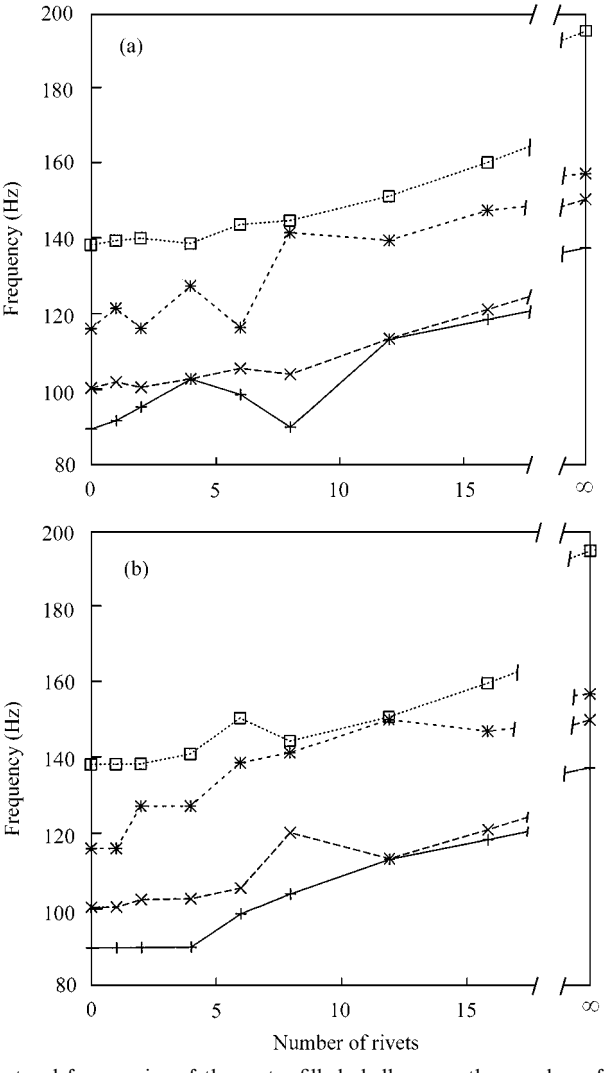

Figure 11. First four natural frequencies of the water-filled shell versus the number of rivets (clamped arcs): (a) symmetric modes; (b) antisymmetric modes.

shell. This is due to the largely increased mass of the system due to the added virtual mass introduced by the contained water.

6.3. Shells on Partial Elastic Bed or with an Intermediate Constraint

The same shell studied in the previous section is considered here. Initially $3 \times 20 \times 24$ modes are considered in the expansion, where 19 is the maximum number of circumferential waves and 24 is the maximum number of axial half-waves. Figure 12 shows the first two modes of the clamped empty shell with an almost rigid central bed, ring-shaped, of width $L/5$. The stiffness of the elastic bed is 10^{10} N/m^3.

Figure 13 shows the first two symmetric and antisymmetric modes of the clamped empty shell with an almost-rigid central bed, limited in both angular and axial directions, of

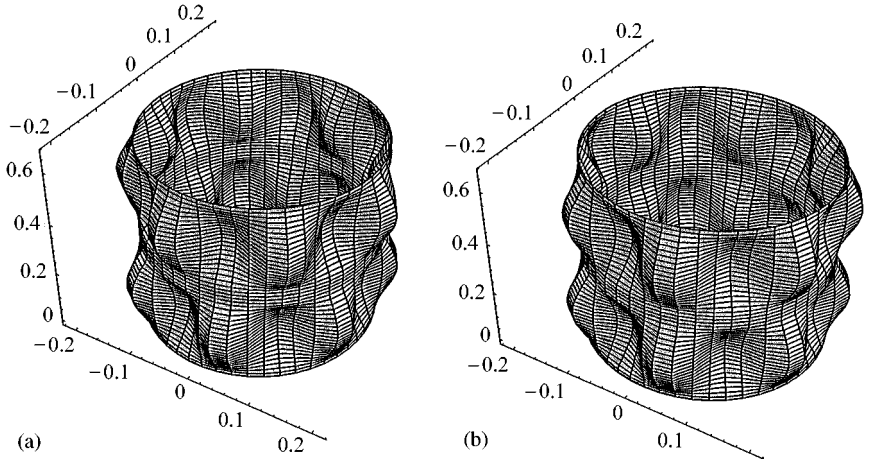

Figure 12. Modes of the clamped empty shell with an almost rigid central ring: (a) first mode, 630 Hz; (b) second mode, 646 Hz.

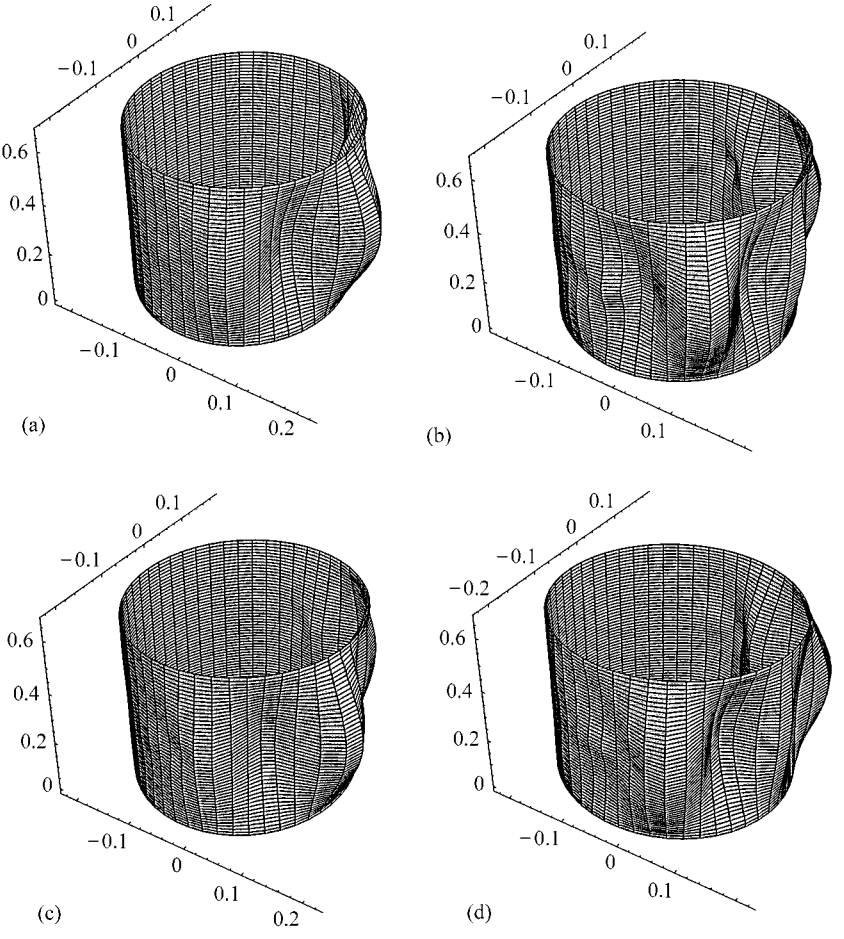

Figure 13. Modes of the clamped empty shell with an almost rigid central bed limited in the axial and angular directions: (a) first symmetric mode, 317 Hz; (b) second symmetric mode, 404 Hz; (c) first antisymmetric mode, 318 Hz; (d) second antisymmetric mode, 417 Hz.

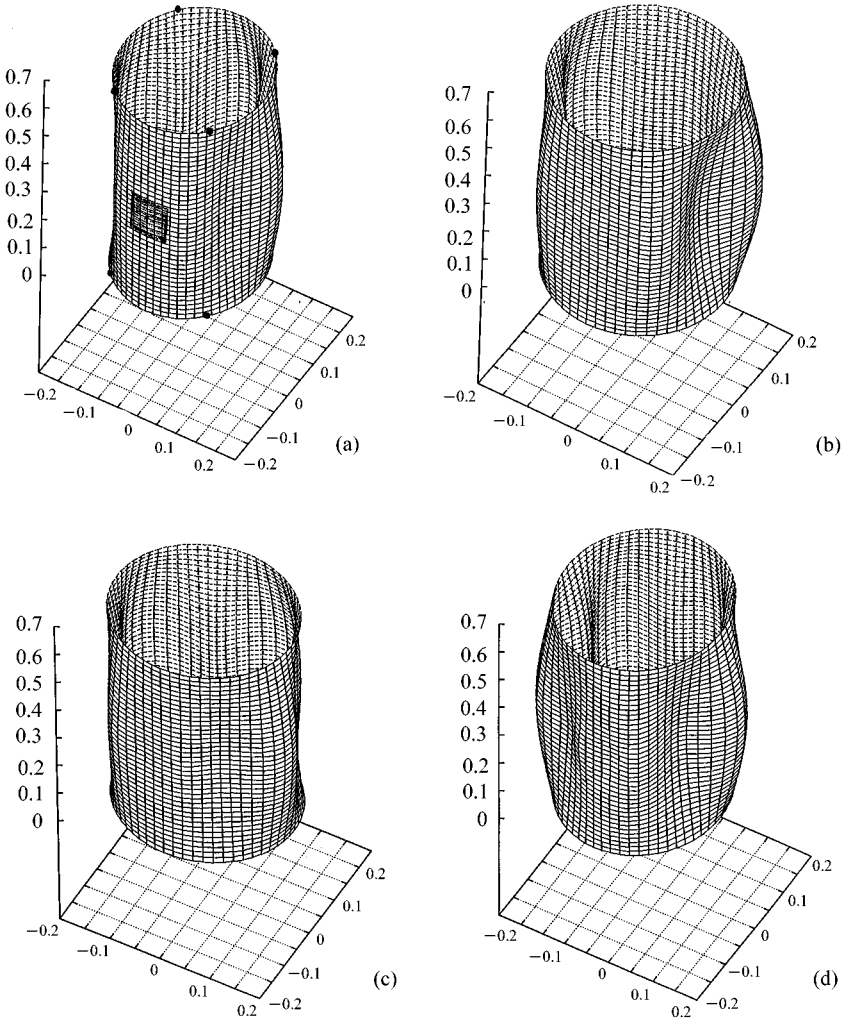

Figure 14. Modes of the water-filled shell with an almost rigid central bed limited in the axial and angular directions and edge-springs on four arcs; positions of rivets and elastic bed are indicated: (a) first symmetric mode, 98 Hz; (b) second symmetric mode, 110 Hz; (c) first antisymmetric mode, 92.8 Hz; (d) second antisymmetric mode, 113 Hz.

dimension $L/5 \times 180^\circ$. The stiffness of the elastic bed is 10^{10} N/m^3 and corresponds to an almost-rigid intermediate constraint on the whole bed extension. Results are obtained with $3 \times 32 \times 21$ modes in the mode expansion, where 31 is the maximum number of circumferential waves and 21 is the maximum number of longitudinal half-waves.

6.4. Water-Filled, Riveted Shells on Partial Elastic Bed

The individual effects previously investigated are combined to study a water-filled ($\rho_F = 1000$ kg/m^3) shell with four rivets and elastic bed of partial angular and longitudinal extension. The shell with the same dimension and material properties as the one in Sections 6.2 and 6.3 is considered. In particular, the shell is assumed to be constrained by springs of stiffness $\tilde{k} = 10^8$ N/m^2 and $c = 10^7$ N at four equispaced arcs of angular

amplitude of 3.6° at each shell ends, away from the angular origin $\theta = 0$. Moreover, an elastic bed of extension $-30^\circ \leq \theta \leq 30^\circ$, $0{\cdot}4L \times 0{\cdot}6L$ and stiffness $\tilde{b} = 10^{10}\ \mathrm{N/m^3}$ is considered. Results, obtained with $3 \times 32 \times 20$ terms in the mode expansion, are given in Figure 14.

7. CONCLUSIONS

Circular cylindrical shells with nonuniform edge constraints are investigated, including riveted shells. Moreover, complicating effects due to contained inviscid fluid, elastic bed of partial longitudinal and angular extensions, intermediate constraints and added mass are considered. The solution is obtained by using the Rayleigh–Ritz method with a simple and systematic choice of admissible functions which are the eigenfunctions of the closest, simple problem extracted from the one considered. In particular, the problem extracted is the simply supported shell and any additional constraint can be studied. The convergence of the method is numerically investigated and the effect of the number of rivets (clamped arcs) on shell modes is studied.

ACKNOWLEDGEMENTS

This research was partially supported by a grant of the Italian Space Agency (ASI).

References

Amabili, M. 1996 Free vibration of a fluid-filled circular cylindrical shell with lumped masses attached, using the receptance method. *Shock and Vibration* **3,** 159–167.

Amabili, M. 1997 Ritz method and substructuring in the study of vibration with strong fluid–structure interaction. *Journal of Fluids and Structures* **11,** 507–523.

Amabili, M. 1999 Vibrations of circular tubes and shells filled and partially immersed in dense fluids. *Journal of Sound and Vibration* **221,** 567–585.

Amabili, M. & Dalpiaz, G. 1997 Free vibrations of cylindrical shells with non-axisymmetric mass distribution on elastic bed. *Meccanica* **32,** 71–84.

Amabili, M. & Garziera, R. 1999 A technique for the systematic choice of admissible functions in the Rayleigh–Ritz method. *Journal of Sound and Vibration* **224,** 519–539.

Amabili, M., Païdoussis, M. P. & Lakis, A. A. 1998 Vibrations of partially filled cylindrical tanks with ring-stiffeners and flexible bottom. *Journal of Sound and Vibration* **213,** 259–299.

Amabili, M., Pierandrei, R. & Frosali, G. 1997 Analysis of vibrating circular plates having non-uniform constraints using the modal properties of free-edge plates: application to bolted plates. *Journal of Sound and Vibration* **206,** 23–38.

Cheng, L. 1994 Fluid-structural coupling of a plate-ended cylindrical shell: vibration and internal sound field. *Journal of Sound and Vibration* **174,** 641–654.

Cheng, L. & Nicolas, J. 1992 Free vibration analysis of a cylindrical shell-circular plate system with general coupling and various boundary conditions. *Journal of Sound and Vibration* **155,** 231–247.

Cheung, Y. K. & Zhou, D. 1999 The free vibration of tapered rectangular plates using a new set of beam functions with the Rayleigh–Ritz method. *Journal of Sound and Vibration* **223,** 703–722.

Forsberg, K. 1964 Influence of boundary conditions on the modal characteristics of thin cylindrical shells. *AIAA Journal* **2,** 2150–2157.

Fu, Y. M. & Chia C. Y. 1993 Non-linear vibration and postbuckling of generally laminated circular cylindrical thick shells with non-uniform boundary conditions. *International Journal of Non-Linear Mechanics* **28,** 313–327.

Ilanko, S. & Dickinson, S. M. 1999 Asymptotic modelling of rigid boundaries and connections in the Rayleigh–Ritz method. *Journal of Sound and Vibration* **219,** 370–378.

Jézéquel, L. 1983 Structural damping by slip in joints. *ASME Journal of Vibration, Acoustics, Stress and Reliability in Design* **105,** 497–504.

Koval, L. R. & Cranch, E. T. 1962 On the free vibrations of thin cylindrical shells subjected to an initial static torque. *Proceedings of the 4th U.S. National Congress of Applied Mechanics*, Vol. 1, pp. 107–117.

LEISSA, A. W. 1973 *Vibration of Shells*, NASA SP-288. Washington, DC: Government Printing Office. Now available from The Acoustical Society of America, 1993.
LEISSA, A. W., LAURA, P. A. A. & GUTIERREZ, R. H. 1979 Transverse vibrations of circular plates having non-uniform edge constraints. *Journal of the Acoustical Society of America* **66,** 180–184.
LOVEDAY, P. W. & ROGERS, C. A. 1998 Free vibration of elastically supported thin cylinders including gyroscopic effects. *Journal of Sound and Vibration* **217,** 547–562.
PAÏDOUSSIS, M. P. & LAKIS, A. A. 1972 Vibration characteristics of cylindrical shells with several axially equispaced constraints. *Journal of Sound and Vibration* **24,** 51–62.
SHIN, Y. S., IVERSON, J. C. & KIM, K. S. 1991 Experimental studies on damping characteristics of bolted joints for plates and shells. *ASME Journal of Pressure Vessel Technology* **113,** 402–408.
SOEDEL, W. 1993 *Vibrations of Shells and Plates*, 2nd edition. New York: Marcel Dekker.
VRONAY, D. F. & SMITH, B. L. 1970 Free vibration of circular cylindrical shells of finite length. *AIAA Journal* **8,** 601–603.
YUAN, J. & DICKINSON, S. M. 1994 The free vibration of circularly cylindrical shell and plate systems. *Journal of Sound and Vibration* **175,** 241–263.

APPENDIX: FLÜGGE THEORY OF SHELLS

The coefficients K_i in equation (2), for $i = 0, 1, 2$, according to the Flügge theory of shells are (Leissa 1973)

$$K_2 = 1 + \frac{3 - \nu}{2}(n^2 + \lambda^2) + k(n^2 + \lambda^2)^2, \tag{A1}$$

$$K_1 = \frac{1 - \nu}{2}\left[(3 + 2\nu)\lambda^2 + n^2 + (n^2 + \lambda^2)^2 + \frac{3 - \nu}{1 - \nu}k(n^2 + \lambda^2)^3\right], \tag{A2}$$

$$K_0 = \frac{1 - \nu}{2}\{(1 - \nu^2)\lambda^4 + k(n^2 + \lambda^2)^4 + k[2(2 - \nu)\lambda^2 n^2 + n^4 - 2\nu\lambda^6 - 6\lambda^4 n^2 - 2(4 - \nu)\lambda^2 n^4 - 2n^6]\}, \tag{A3}$$

where $\lambda = m\pi R/L$ and $k = h^2/(12R^2)$.

The mode shape coefficients A_{nmj} and B_{nmj} are computed by the following linear system for the Flügge theory of shells (Leissa 1973):

$$\begin{bmatrix} -\lambda^2 - (1 + k)\dfrac{1 - \nu}{2}n^2 + \Omega^2 & \dfrac{1 + \nu}{2}\lambda n \\ \dfrac{1 + \nu}{2}\lambda n & -n^2 - \dfrac{1 - \nu}{2}\lambda^2(1 + 3k) + \Omega^2 \end{bmatrix} \begin{bmatrix} A_{nmj} \\ B_{nmj} \end{bmatrix} = \begin{bmatrix} -\nu\lambda + k\lambda\left(\lambda^2 + \dfrac{1 - \nu}{2}n^2\right) \\ n + \dfrac{3 - \nu}{2}k\lambda^2 n \end{bmatrix}. \tag{A4}$$